

# Chapter 21

## Inkjet Printed Chemical Sensors

F. Villani, I. A. Grimaldi, T. Polichetti, E. Massera,  
A. De Girolamo Del Mauro and G. Di Francia

**Abstract** Polymer nanocomposites (PNCs) represent a new class of sensing materials for volatile organic compounds (VOCs) detection. These materials can be simply processed by inkjet printing (IJP) technique, an emerging technology that has assumed a key role in the field of electronics wherever replacing conventional rigid substrates with flexible ones is required. In the present work, we fabricated PNCs chemical sensors inkjet printing a polystyrene (PS)/carbon black (CB) composite based ink on different substrates, flexible and not, such as polyethylene terephthalate (PET), glass and alumina. The sensors responses have been analyzed upon exposure to acetone organic vapors and compared in terms of sensitivity, response time and limit of detection.

### 21.1 Introduction

Polymer nanocomposites (PNCs) are a new category of materials consisting of an insulating polymer matrix where nanosized inorganic fillers are dispersed in. They combine the simple processability of polymers together with the conductivity and mechanical-stability properties of nanoparticles. The resultant hybrid system is attractive in several research sectors. Chemiresistors based on conductive PNCs are being used in sensing applications thanks to their simple transduction mechanism based on a change of their electric properties when they come into contact with a specific substance; in fact, due to the solvent absorption the polymer volume changes (swelling) [1–3], correspondingly the volumetric fraction of the conductive nanoparticles decreases [4], which reflects as a change of the electrical

---

F. Villani (✉) · I. A. Grimaldi · T. Polichetti · E. Massera · A. De Girolamo Del Mauro ·  
G. Di Francia  
ENEA Research Center, P.le E. Fermi 1, 80055, Portici (Na), Italy  
e-mail: fulvia.villani@enea.it

conductivity. PNCs can be easily processed by techniques such as spin-coating or drop-casting and, recently, also by inkjet printing (IJP) technology, rapidly emerged as an innovative technique for the deposition of a wide variety of materials [5–8]. The advantages of IJP over the aforementioned techniques lie in its patterning capability, the efficient use of material, the reduced waste products and low cost of the process, and its potential for printing at ambient temperature with no contact or vacuum on both non-flexible and flexible substrates. As concerning this last item, the IJP technology has assumed a main role in the field of electronics wherever it is required to replace conventional non-flexible substrates with flexible ones. In the present work, VOCs chemical sensors have been fabricated by printing the PS/CB nanocomposite on different substrates, such as PET, glass, and alumina. The effect of the substrate morphology on the printed film quality and, hence, on the device performances has been investigated.

## 21.2 Experimental

The employed substrates ( $5 \times 5 \text{ mm}^2$ ) were PET, glass and alumina. The electrodes have been realized by commercial sputtered ITO for both PET and glass substrates, and by evaporated Au in the case of alumina. The geometry of interdigitated contacts has been always defined patterning ITO or Au by conventional photolithography process. The sensing material is a nanocomposite composed by atactic polystyrene (PS, Sigma–Aldrich) and carbon black (CB, Black Pearls 2000-Cabot Co.). The PS polymer matrix (80 mg) has been dissolved in *n*-Methyl-2-pyrrolidinone (NMP) and the CB conductive filler (20 mg) has been dispersed in the polymeric solution (0.5 wt%) by means of ultrasonic bath. Bigger agglomerates have been removed by filtering the PS/CB suspension through a 0.2- $\mu\text{m}$  filter. The final dispersion has been employed as ink and printed onto 50°C heated electrodes/substrate system. Sequences of overlapping droplets to create a line transverse to the fingers of the interdigitated electrodes have been printed by means of a piezoelectric Drop on Demand print-head (70  $\mu\text{m}$  opening nozzle). The printed material has been investigated by optical micrographs and SEM analysis. The sensor response has been analyzed upon exposure to acetone organic vapors at different concentrations in a test chamber placed in a thermostatic box at controlled temperature and humidity.

## 21.3 Results and Discussion

Overlapped drops of nanocomposite based ink have been IJ-printed on patterned-ITO/PET and /glass substrates. The optical micrographs of the printed material, reported in Fig. 21.1, highlight the different wettability of the investigated ink/substrate systems. The spreading of the printed droplet depends on both substrate

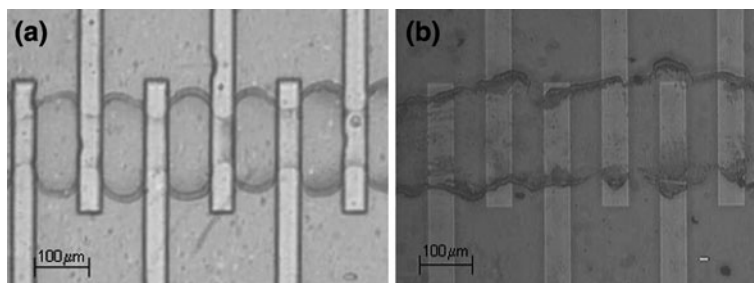


**Fig. 21.1** Optical micrographs of the sensing material printed on PET (a) and glass (b) substrates

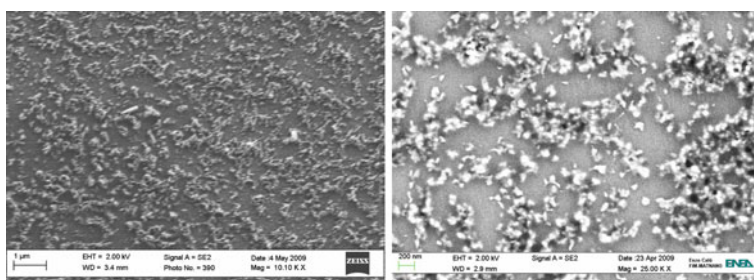


**Fig. 21.2** SEM images of PS/CB nanocomposite based ink printed on PET (*left*) and glass (*right*) substrates

surface energies and roughness. In particular, ITO/PET higher roughness (average roughness 8.6 nm) induces a more regular printed pattern as compared to the profile printed onto ITO/glass (average roughness 2.4 nm). SEM images exhibit percolative paths of the conductive filler uniformly distributed on both the substrates (Fig. 21.2). The chemical sensor devices have been fabricated according to three different configurations with mono-, three- and five-overlapped layers with the aim of investigating the thickness effect on the sensor performances. By comparison, the same configurations have been performed on the interdigitated-Au/alumina system, extensively investigated in previous works [7, 8]. The devices electrical responses to acetone vapors are shown in Fig. 21.3a, b and c for PET, glass and alumina substrates, respectively. The parameters that characterize the sensor performances, such as base resistance, sensitivity, lower detection limit (LdL) and time response, are summarized in Tables 21.1, 21.2 and 21.3 for each substrate. For all the substrates, the results indicate that the dynamic responses of the five-layers sensors, the devices with smaller base resistance, are characterized by higher sensitivity and minimum LdL values as compared with the sensors fabricated with a lower layers number. Moreover, the five-layers devices electrical responses do not reach the saturation condition at higher analyte concentration due to the change of the adsorption kinetic of the systems characterized by lower

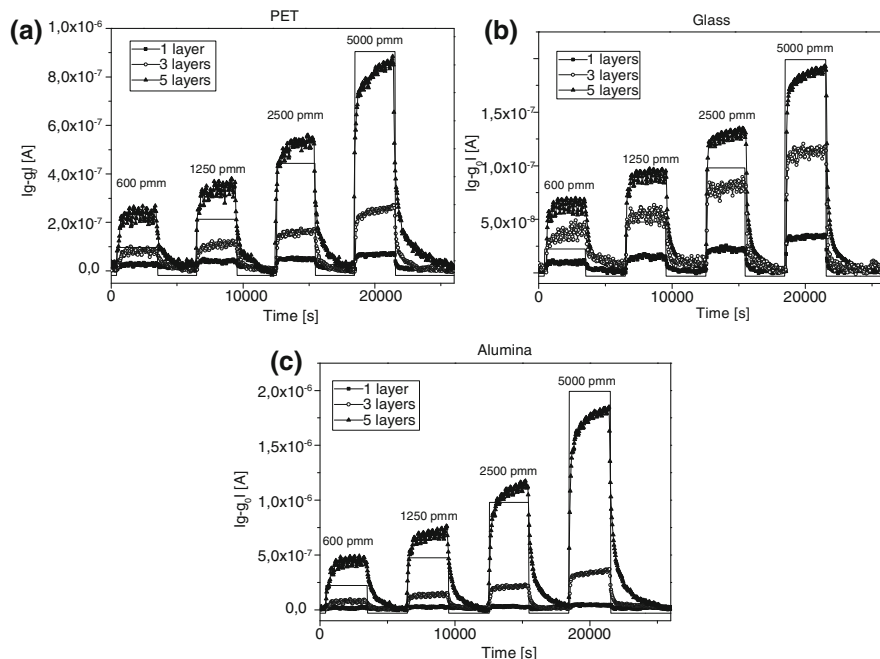


**Fig. 21.3** Electrical responses to acetone vapors of one-, three- and five-layers sensors on PET (a), glass (b) and alumina (c)

**Table 21.1** Electrical response parameters of the sensors on PET

PET	Resistance (K $\Omega$ )	Sensitivity (S/ppm)	Lower detection Limit (LdL) (ppm)	Time response (s)
One layer	230	8.86e-12	800	200
Three layers	70	3.86e-11	300	200
Five layers	17	1.36e-10	100	250

**Table 21.2** Electrical responses parameters of the sensors on glass

Glass	Resistance (K $\Omega$ )	Sensitivity (S/ppm)	Lower detection Limit (LdL) (ppm)	Time response (s)
one layer	300	5.42e-12	300	100
Three layers	105	1.7e-11	200	100
Five layers	90	2.9e-11	50	100

surface/volume ratio. Finally, it is evident that the response times of the sensors printed on PET are slightly higher than those fabricated on the other substrates. This behaviour can be attributed to the different morphology of the printed material, which is directly correlated to the ink-substrate interaction.

**Table 21.3** Electrical responses parameters of the sensors on alumina

Alumina	Resistance (K $\Omega$ )	Sensitivity (S/ppm)	Lower detection Limit (LdL) (ppm)	Time response (s)
One layer	200	6.0e-12	2000	100
three layers	40	5.8e-11	86	100
five layers	9	3,05e-10	50	100

## 21.4 Conclusions

In the present work, we fabricated polymer nanocomposites chemical sensors on different, flexible and not, substrates and investigated how their performances are related to substrate wettability. The sensing material has been deposited by means of ink-jet printing technique in three different configurations, one-, three- and five-layers. The results indicate that the dynamic responses of the five-layers sensors have got the higher sensitivity and minimum LdL values, regardless of substrate. Moreover, the sensors printed onto PET are slower than the other devices probably due to the different morphology of the printed material.

**Acknowledgments** This work was supported by the TRIPODE project (DM 20160) financed by the Ministero dell'Università e della Ricerca (MUR).

## References

1. Chatzandroulis S, Goustouridis D, Raptis I (2005) Characterization of polymer films for use in bimorph chemical sensors. *J Phys Conf Series* 10:297
2. Goustouridis D, Manoli K, Chatzandroulis S, Sanopoulou M, Raptis I (2005) Characterization of polymer layers for silicon micromachined bilayer chemical sensors using white light interferometr. *Sens Actuators B* 111:549–554
3. Convertino A, Leo G, Tamborra M, Sciancalepore C, Striccoli M, Curri ML, Agostano A (2007) TiO<sub>2</sub> colloidal nanocrystals functionalization of PMMA: a tailoring of optical properties and chemical adsorption. *Sens Actuators B* 126:138–143
4. Carrillo A, Martin-Dominguez IR, Marquez-Lucero A (2006) Modeling and experimental testing of the effect of solvent absorption on the electric properties of styrene butadiene rubber/carbon black chemical sensors. *Sens Actuators B* 113:477–486
5. Ballarin B, Fraleoni-Morgera A, Frascaro D, Marazzita S, Piana C, Setti L (2004) Thermal inkjet microdeposition of PEDOT:PSS on ITO-coated glass and characterization of the obtained film. *Synth Met* 146:201–205
6. Yoshioka Y, Jabbour GE (2006) Desktop inkjet printer as a tool to print conducting polymers. *Synth. Met* 156:779–783
7. Loffredo F, Burrasca G, Quercia L, Della Sala D (2007) Gas sensor devices obtained by ink-jet printing of polyaniline suspension. *Macromol Symp* 247:357–363
8. Loffredo F, De Girolamo Del Mauro A, Burrasca G, La Ferrara V, Quercia L, Massera E, Di Francia G, Della Sala D (2009) Ink-jet printing technique in polymer/carbon black sensing device fabrication. *Sens Actuators B* 143:421–429